

Quantum estimation of rotational speed in optomechanics

Hao Li(李浩), and Jiong Cheng(程泂)
Citation: Chin. Phys. B, 2023, 32 (**10**): 100602. DOI: 10.1088/1674-1056/ace3b7
Journal homepage: http://cpb.iphy.ac.cn; http://iopscience.iop.org/cpb

What follows is a list of articles you may be interested in

Multilevel atomic Ramsey interferometry for precise parameter estimations

X N Feng(冯夏宁) and L F Wei(韦联福)
Chin. Phys. B, 2021, 30 (**12**): 120601. DOI: 10.1088/1674-1056/ac0527

Pre- and post-selected measurements with coupling-strength-dependent modulation

Zhaoxue Li(李兆雪), Jiangdong Qiu(邱疆冬), Linguo Xie(谢林果), Lan Luo(罗兰), Xiong Liu(刘雄), Zhiyou Zhang(张志友), Changliang Ren(任昌亮), JingLei Du(杜惊雷)
Chin. Phys. B, 2019, 28 (**3**): 030602. DOI: 10.1088/1674-1056/28/3/030602

Quantum parameter estimation in a spin-boson dephasing quantum system by periodical projective measurements

Le Yang(杨乐), Hong-Yi Dai(戴宏毅), Ming Zhang(张明)
Chin. Phys. B, 2018, 27 (**4**): 040601. DOI: 10.1088/1674-1056/27/4/040601

Optimal quantum parameter estimation of two-qutrit Heisenberg *XY* chain under decoherence

Hong-ying Yang(杨洪应), Qiang Zheng(郑强), Qi-jun Zhi(支启军)
Chin. Phys. B, 2017, 26 (**1**): 010601. DOI: 10.1088/1674-1056/26/1/010601

Enhancing the precision of phase estimation by weak measurement and quantum measurement reversal

He Zhi (贺志), Yao Chun-Mei (姚春梅)
Chin. Phys. B, 2014, 23 (**11**): 110601. DOI: 10.1088/1674-1056/23/11/110601

Quantum estimation of rotational speed in optomechanics

Hao Li(李浩) and Jiong Cheng(程泂)[†]

Department of Physics, Ningbo University, Ningbo 315211, *China*

(Received 30 March 2023; revised manuscript received 5 June 2023; accepted manuscript online 4 July 2023)

We study the quantum Fisher information (QFI) of the angular velocity of rotation in an optomechanical system. Based on the Gaussian measurements method, we derive the explicit form of a single-mode Gaussian QFI, which is valid for arbitrary angular velocity of rotation. The information about the angular velocity to be measured is contained in the optical covariance matrix, which can be experimentally determined via homodyne measurement. We find that QFI increases rapidly when driving the system close to the unstable boundary. This result can be attributed to the strong nonlinearity of the system at the unstable boundary. Our results indicate the possibility of using an optomechanical system for high precision detection of the angular velocity of rotation.

Keywords: optomechanical system, Fisher information

PACS: 06.30.Gv, 42.50.Lc, 42.50.–p **DOI:** 10.1088/1674-1056/ace3b7

1. Introduction

Quantum measurement is an important technology in quantum information science.[1–4] The bound of the detection accuracy is essentially due to Heisenberg uncertainty relationship.[5,6] Quantum parameter estimation can be used to find this limit in the precision of quantum measurement.[1,7] For a given measurement, the maximal achievable precision of the estimation is determined by the so-called Fisher information.[8] Many effective methods have been proposed to optimize measurements based on Fisher information, e.g., Fisher-information-based estimation of optomechanical coupling strengths,[9] projective photon-counting measurement of single photons,[10] quantum estimation methods for quantum illumination,[11] and so on.

In the field of quantum measurement, the ability to detect the properties of a mechanical object at the quantum precision limit has attracted significant attention because it can show the boundary of quantum-classical transition,[12,13] macroscopic quantum effect[14–16] and so on. As a potential platform for precise measurement,[17–19] an optomechanical system has natural advantages[20–28] because a quantized light field is very sensitive to mechanical motion.[18,29–31] With the help of optomechanical coupling, a quantum detector can detect gravitational waves,[17,32–34] tiny masses,[35,36] tiny displacements,[37,38] and weak fields with greater precision than the classical detectors.[30] Among them, the measurement of angular velocity has attracted considerable attention, and is used as the basis of a gyroscope.[39,40] Meanwhile, a mechanical object is naturally sensitive to centrifugal force when rotating at a certain angular velocity. Related detection schemes have also been proposed in optomechanical systems.[40] By means of semi-classical treatment, the angular velocity can be introduced by the coefficients of the system operator, or by an effective drive.[41]

The detection limit of the system has not yet been fully discussed in these studies. We note that the combination of the optomechanical system with QFI allows us to estimate the parameters of the system. In Ref. [9], the designed quadrature measurements allow very accurate estimation of optomechanical coupling strengths. This offers a possibility to estimate the angular velocity by using quantum metrology with the platform of optomechanical system. QFI can be used to quantify this estimation and give the limit. Therefore, in this study we use QFI to investigate the limit of optomechanical system in angular velocity detection.

This paper is organized as follows. In Section 2, we introduce the system and derive the dynamical evolution of the Hamiltonian. In Section 3, we discuss the relationship between covariance matrix and QFI under Gaussian measurement. The numerical results and the corresponding discussion are given in Section 4. Finally, a summary is given in Section 5.

2. Model

We consider a cavity optomechanical system that consists of a Fabry–Pérot cavity with frequency $\omega_{\rm c}$ and a mechanical resonator with frequency $\omega_{\rm m}$. The cavity is driven by a coherent laser with driving strength ε and center frequency ω_0. The system is fixed on a rotating table with angular velocity Ω (see Fig. 1). The Hamiltonian of the system reads[42,43]

$$\hat{H} = \hbar\omega_{\rm c}\hat{a}^{\dagger}\hat{a} + \frac{1}{2}\hbar\omega_{\rm m}(\hat{p}^2+\hat{q}^2) - \hbar G_0\hat{a}^{\dagger}\hat{a}\hat{q} - \frac{\hbar}{2\omega_{\rm m}}\Omega^2(R+\hat{q})^2 + {\rm i}\hbar\varepsilon(\hat{a}^{\dagger}{\rm e}^{-{\rm i}\omega_0 t} - \hat{a}{\rm e}^{{\rm i}\omega_0 t}), \quad (1)$$

[†]Corresponding author. E-mail: chengjiong@nbu.edu.cn

© 2023 Chinese Physical Society and IOP Publishing Ltd

where the first and second terms describe the energy of the cavity and mechanical oscillator, respectively. The third term is the radiation pressure induced optomechanical interaction with coupling strength $G_0 = (\omega_c/L)\sqrt{\hbar/(m\omega_m)}$. The fourth term describes the kinetic energy of the oscillator due to the rotation of the turntable. The dimensionless rotational inertia satisfis $\hat{I} = \frac{\hbar}{\omega_m}(R+\hat{q})^2$ with $R = R_0/\sqrt{\hbar/(m\omega_m)}$, where R_0 is the distance between the center of the turntable and the oscillator. The last term is the input driving laser with $\varepsilon = \sqrt{2P\kappa/(\hbar\omega_L)}$, where P is the laser power.

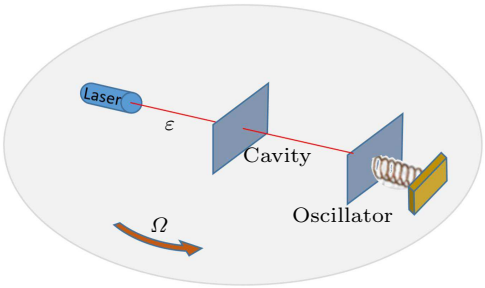


Fig. 1. Schematic diagram of optomechanical gyroscope. A cavity optomechanical system is placed on a rotating platform with its input end located at the center of the platform. The platform is rotating with angular velocity Ω.

In the frame rotating at the laser frequency ω_0, we can obtain the following quantum Langevin equations:[44–46]

$$\dot{\hat{q}} = \omega_m \hat{p}, \tag{2a}$$

$$\dot{\hat{p}} = -(\omega_m - \frac{\Omega^2}{2\omega_m})\hat{q} - \gamma_m \hat{p} + G_0 \hat{a}^\dagger \hat{a} + \frac{\Omega^2}{\omega_m} R + \hat{\xi}, \tag{2b}$$

$$\dot{\hat{a}} = -(\kappa + i\Delta)\hat{a} + iG_0 \hat{a}\hat{q} + \varepsilon + \sqrt{2\kappa}\hat{a}_{in}, \tag{2c}$$

where $\Delta = \omega_c - \omega_0$ is the detuning between the cavity field and the driving laser. $\hat{\xi}$ and $\hat{a}_{in}$ are the noise operators of the mechanical and optical modes, respectively. If $\omega_m \gg \Omega$, then the first term in Eq. (2b) reduces to $-\omega_m \hat{q}$. Under strong driving conditions, one can linearize the equations of motion around the steady-state values, i.e., $\hat{O} = O + \delta\hat{O}$, where O and $\delta\hat{O}$ are the classical mean value and quantum fluctuation of $\hat{O}$. The classical steady-state amplitude of the cavity field satisfies $\alpha_s = \varepsilon/(\kappa + i\bar{\Delta})$, where $\bar{\Delta} = \Delta - \frac{G_0^2|\alpha_s|^2}{\omega_m} - \frac{G_0\Omega^2 R}{\omega_m^2}$. Then, the linearized equations of motion describing the quantum fluctuations are given by

$$\delta\dot{\hat{a}} = -(\kappa + i\Delta)\delta\hat{a} + iG_0\alpha\delta\hat{q} + \sqrt{2\kappa}\delta\hat{a}_{in}, \tag{3a}$$

$$\delta\dot{\hat{q}} = \omega_m \delta\hat{p}, \tag{3b}$$

$$\delta\dot{\hat{p}} = -\omega_m\delta\hat{q} - \gamma_m\delta\hat{p} + G_0(\alpha^*\delta\hat{a} + \alpha\delta\hat{a}^\dagger) + \hat{\xi}. \tag{3c}$$

Here, $\delta\hat{a}$, $\delta\hat{q}$ and $\delta\hat{p}$ are the quantum fluctuation operators of the system. By introducing the vector of quantum fluctuations $u(t) = (\delta\hat{X}, \delta\hat{Y}, \delta\hat{q}, \delta\hat{p})^T$, with $\delta\hat{X} = (\delta\hat{a} + \delta\hat{a}^\dagger)/\sqrt{2}$, $\delta\hat{Y} = (\delta\hat{a} - \delta\hat{a}^\dagger)/(i\sqrt{2})$, one can rewrite the equations of the quantum fluctuations by

$$\dot{u}(t) = Au(t) + \eta(t), \tag{4}$$

where $\eta(t) = (\sqrt{2\kappa}\delta\hat{X}_{in}, \sqrt{2\kappa}\delta\hat{Y}_{in}, 0, \hat{\xi}(t))^T$ is the noise vector, and the drift matrix A reads

$$A = \begin{pmatrix} -\kappa & \bar{\Delta} & -G_0Y_s & 0 \\ -\bar{\Delta} & -\kappa & G_0X_s & 0 \\ 0 & 0 & 0 & \omega_m \\ G_0X_s & G_0Y_s & -\omega_m & -\gamma_m \end{pmatrix}. \tag{5}$$

Here, $X_s = \sqrt{2}\mathrm{Re}\alpha_s$, and $Y_s = \sqrt{2}\mathrm{Im}\alpha_s$. The formal solution of Eq. (4) can be written as

$$u(t) = \exp(At)u(0) + \int_0^t \exp(As)\eta(t-s)\,\mathrm{d}s. \tag{6}$$

The system is stable and reaches its steady state when all of the eigenvalues of A have a negative real part. The stability conditions can then be derived by applying the Routh–Hurwitz criterion. From now on, we assume that the stability conditions are satisfied. If the mechanical quality factor is large enough $\mathcal{Q} = \omega_m/\gamma_m \gg 1$, then $\hat{\xi}(t)$ is delta-correlated[45]

$$(\langle\hat{\xi}(t)\hat{\xi}(t') + \hat{\xi}(t')\hat{\xi}(t)\rangle)/2 \backsimeq \gamma_m(2\bar{n}_{th}+1)\delta(t-t'), \tag{7}$$

where $\bar{n}_{th} = [\exp(\frac{\hbar\omega_m}{k_B T}) - 1]^{-1}$ is the mean thermal excitation number. In the steady-state limit, the covariance matrix can be defined as $\sigma_s = (\langle u_i(\infty)u_j(\infty) + u_j(\infty)u_i(\infty)\rangle)/2$. As a consequence, it satisfies the following Lyapunov equation:[47]

$$A\sigma_s + \sigma_s A^\dagger = -D, \tag{8}$$

where D is the noise matrix

$$D = \begin{pmatrix} \kappa & 0 & 0 & 0 \\ 0 & \kappa & 0 & 0 \\ 0 & 0 & 0 & 0 \\ 0 & 0 & 0 & \gamma_m(2\bar{n}_{th}+1) \end{pmatrix}. \tag{9}$$

The parameter to be measured, i.e., Ω, is encoded in the drift matrix A, which determines the steady-state covariance matrix. Therefore, by detecting the output field, one can obtain information about the covariance matrix, which may help us to estimate the value of the angular velocity Ω.

Now we take the covariance matrix of our model in this result. The solution of Eq. (8) can be expressed in the following matrix form:

$$\sigma_s = \begin{pmatrix} \sigma_m & \sigma_c \\ \sigma_c^T & \sigma_L \end{pmatrix}. \tag{10}$$

Here σ_m (σ_L) corresponds to the covariance matrix of the mechanical (optical) subsystem, while σ_c brings about the optomechanical correlations. In this system, the output optical signals can easily be measured through optical homodyne detection, and therefore we can use the input–output relationship $\delta a_{out} = \sqrt{2\kappa}\delta a - \delta a_{in}$ to obtain the optical output matrix $\sigma_{L,out}$.

3. QFI of optomechanics with Gaussian measurements

In quantum metrology, the Cramér–Rao bound[48] is one of the most important results in parameter-estimation theory. For an unbiased estimator, the Cramér–Rao bound of the parameter θ to be estimated reads

$$\Delta\theta_{\mathrm{CR}} = \frac{1}{\sqrt{nF(\theta)}}, \tag{11}$$

where n is the number of measurements. For continuous variables, $F(\theta)$ reads

$$F(\theta) = \int_{\mu} \frac{1}{P(\mu|\theta)} \left(\frac{\partial P(\mu|\theta)}{\partial\theta}\right)^2, \tag{12}$$

where $P(\mu|\theta) = \mathrm{Tr}\left[\hat{\Pi}\rho\right]$ is the probability distribution of the outcome μ conditional on the unknown actual value θ of the parameter, which can be obtained under the measurement of POVM operator $\hat{\Pi}$. If the measurement is independent of θ, then the upper bound of the Fisher information is obtained by maximizing Eq. (12) over all possible generalized measurements in quantum mechanics, $I_{\mathrm{Q}} = \max_{\{\hat{\Pi}\}} F \geqslant F$, which is called QFI. So the quantum Cramér–Rao bound $\Delta\theta_{\mathrm{QCR}} \leqslant \Delta\theta_{\mathrm{CR}}$ For all the possible measured observables, the QFI can be defined as[49,50]

$$I_{\mathrm{Q}} = \mathrm{Tr}\left[\rho L^2\right], \tag{13}$$

where L is the symmetric logarithmic derivative (SLD) operator, which satisfy

$$\frac{\mathrm{d}\rho}{\mathrm{d}\theta} = \frac{1}{2}\{L,\rho\}. \tag{14}$$

According to the Gaussian measurements method of QFI,[51] we can derive the following single-mode Gaussian QFI of Ω (the detailed derivations are given in Appendix A):

$$I_{\mathrm{Q}}(\Omega) = \frac{\det\partial_\Omega\sigma_{\mathrm{L,out}}{}^2\mathrm{Tr}\left[(\sigma_{\mathrm{L,out}}/\partial_\Omega\sigma_{\mathrm{L,out}})^2\right] + \frac{1}{2}\det\partial_\Omega\sigma_{\mathrm{L,out}}}{2\det\sigma_{\mathrm{L,out}}{}^2 - \frac{1}{8}}. \tag{15}$$

Thus, the parameter measurement precision can be evaluated through Eq. (15) when the covariance matrix $\sigma_{\mathrm{L,out}}$ is determined. We know that the covariance matrix is a positive semi-definite matrix and its determinant is the product of the eigenvalues of the matrix. Note that the mean values of the linearized fluctuation Eq. (3) is zero. Meanwhile, the system decoherence dynamics are certainly affected by the optomechanical coupling. Thus, according to the Heisenberg uncertainty relation, $\det\sigma_{\mathrm{L,out}} \geq 1/4$. The denominator of Eq. (15) will remain greater than zero. From the above analysis and Eq. (15), it can be found that if the input state is a squeezing state, then QFI can be further improved. The information of the mechanical oscillator is transmitted to the photon via the optomechanical coupling. When Ω increases, the number of photons in the cavity increases correspondingly, and consequently $\delta\hat{X}$ and $\delta\hat{Y}$ also increases. The partial derivative of the covariance matrix with respect to Ω, namely, $\partial_\Omega\sigma_{\mathrm{L,out}}$, then increases. This is the reason why the measurement accuracy of Ω can be improved. Since $\partial_\Omega\sigma_{\mathrm{L,out}}$ should be greater than zero, this guarantees the non-negativity of QFI in Eq. (15).

4. Rotational speed estimation in optomechanical system

In this section, we numerically study the impact of system parameters on QFI. By solving the Lyapunov equation, the output optical covariance matrix is obtained, and then QFI can be determined through Eq. (15). Figure 2 shows the density plot of QFI varies with the laser power P and cavity detuning Δ. To clearly show the distribution characteristics of QFI, we only show the regime that $I_{\mathrm{Q}} > 0.1$ (i.e., the iridescence line between green and white areas). The green area represents the stability regime of the system, while the white area represents the unstable regime. By changing the optical dissipation rate κ, the stability regime has changed markedly, and we note that the large values of QFI always appear at the boundary of the stability regime. Near the unstable regime, the nonlinear effect of the system plays a leading role, which greatly affects the value of QFI. Meanwhile, in the unstable regime, the assumption of steady-state covariance matrix is not valid and the covariance matrix changes abruptly at the boundary. This results in the formation of extreme values of QFI at the boundary. We can also see that the QFI has a lot of local optimum points at the boundary. This indicates a way to improve measurement accuracy, i.e., driving the system close to the unstable regime and finding the global optimum value for QFI. Comparing Figs. 2(a) and 2(b), we find that we can improve the QFI of the angular velocity measurement by increasing the Q factor of the cavity. In Fig. 2(c), we present the partially enlarged drawing of Fig. 2(a), which clearly shows the behavior of QFI near the boundary. This also provides us with a reliable range of parameters for achieving large values of QFI. We plot Fig. 2(d) by fixing the cavity detuning along the boundary. The small peak in (d) indicates the local optimal value of QFI. For our numerical analysis, we take experimentally feasible parameters,[52] which are $m = 6$ ng, $L = 25$ mm, $\omega_{\mathrm{m}}/2\pi = 2.75\times10^5$ Hz, $\gamma_{\mathrm{m}} = 10^{-5}\omega_{\mathrm{m}}$, $\omega_{\mathrm{c}} = 4.8\times10^2$ THz. In addition, we assume that the angular velocity to be measured is $\Omega = 35$ Hz, and the distance between the center of the turntable and the oscillator is $R_0 = 5L$.

In the following, we investigate the sensitivity of the angular velocity. We use blue and red detuned lasers to pump the cavity, and the results are shown in Fig. 3. In Fig. 3(a),

the laser is blue detuned, and we can see that the steady-state region increases as Ω gets larger. In this situation, for $\Omega < 50$ Hz, the required maximum laser power is $P \approx 1$ mW. In the high rotational speed case, the blue detuned laser is

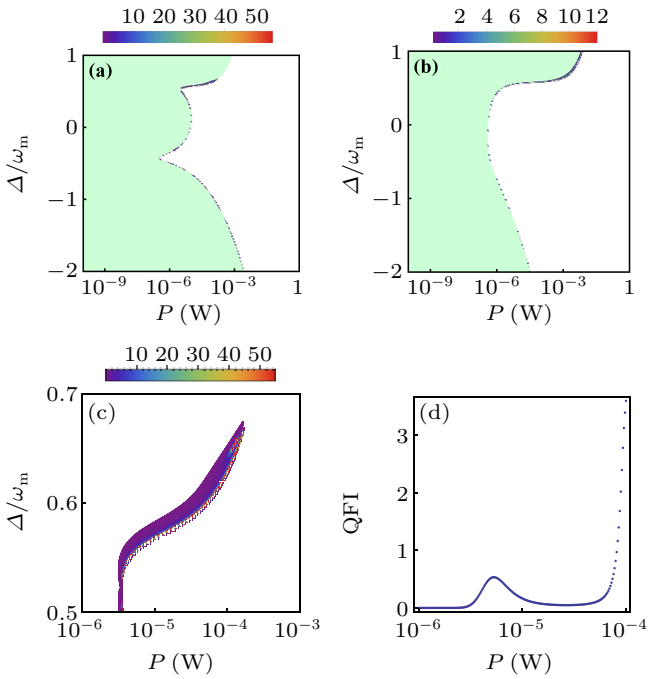


Fig. 2. (a)–(c) Density plot of QFI as a function of laser power P and cavity detuning Δ. (d) QFI as a function of laser power P when Δ is fixed along the boundary. We set $m = 6$ ng, $R_0 = 5L$, $L = 25$ mm, $\omega_m/2\pi = 2.75 \times 10^5$ Hz, $\gamma_m = 10^{-5}\omega_m$, $\omega_c = 4.8 \times 10^2$ THz, $\bar{n}_{th} = 100$, and the rotational speed $\Omega = 35$ Hz. In panels (a) and (b) we keep $\kappa/\omega_m = 0.05$, and 0.5 respectively. The partial enlarged drawing of panel (a) is plotted in panel (c) for $\Delta \sim 0.6$.

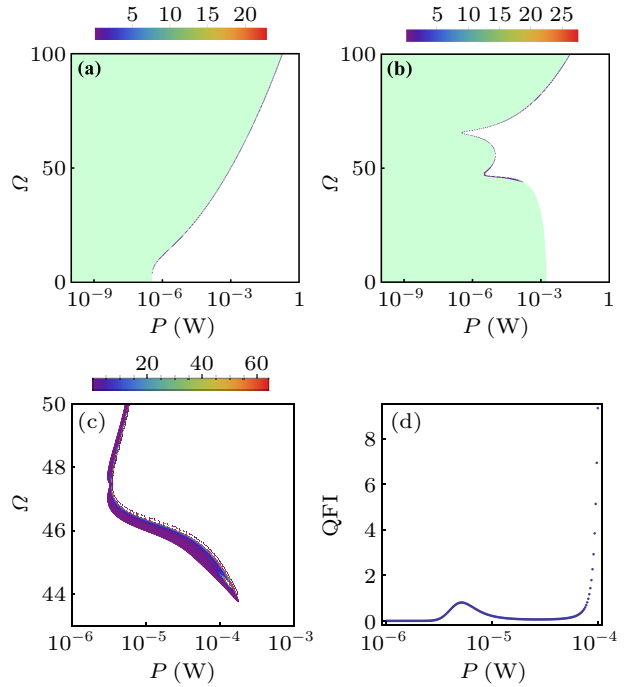


Fig. 3. (a)–(c) Density plot of QFI as a function of the laser power P and angular velocity Ω. (d) QFI as a function of laser power P when Ω is fixed along the boundary. The parameters are the same as in Fig. 2. In panel (a) we keep $\Delta = -1$ and in panel (b) $\Delta = 1$. The partially enlarged drawing of panel (b) is plotted in panel (c) for $\Omega \sim 46$ Hz.

no longer valid and one should modulate the laser to the red detuned regime, which is shown in Fig. 3(b). In (b), the high rotational speed can be measured on the mW scale, while for $\Omega < 50$ Hz the accuracy of the measurement decreased significantly, i.e., QFI < 0.1. The results of Fig. 3 can be understood very clearly because the effective detuning $\bar{\Delta} = \Delta - \frac{G_0^2|\alpha_s|^2}{\omega_m} - \frac{G_0\Omega^2 R}{\omega_m^2}$. For the parameters under consideration, $G_0 R \gg 1$. Then, increasing the angular velocity will effectively decrease the effective detuning, which means that the appropriate regime for our detection scheme is to keep $\bar{\Delta} \approx -1$. We also present the partially enlarged drawing of Fig. 3(b) in Fig. 3(c), which gives us a clear parameter regime for achieving large QFI. The local optimal behavior of QFI is also observed in Fig. 3(d), where the angular velocity is fixed along the boundary.

5. Conclusion

In conclusion, we have studied the QFI of the rotational speed in an optomechanical system. We derived the explicitly single-mode Gaussian QFI for arbitrary angular velocity. Using this result, we find the way to maximum the value of QFI, i.e., driving the system close to the unstable boundary. Our results show that the optomechanical system can be used as a gyroscope, detecting the rotational speed with high precision.

Appendix A: QFI for Gaussian state

In this appendix, by using the approach proposed in Ref. [51], we will give a detailed derivation of our main result, i.e., Eq. (15). For n-mode Gaussian states, the symmetrically ordered character function is

$$\chi_S(\boldsymbol{\xi}) = \mathrm{tr}(\rho\, e^{i\boldsymbol{r}^T\boldsymbol{\xi}}), \tag{A1}$$

where $e^{i\boldsymbol{r}^T\boldsymbol{\xi}} \equiv D(\boldsymbol{\xi})$ is the shift operator in phase space $D(\boldsymbol{\xi})^\dagger \hat{\boldsymbol{r}} D(\boldsymbol{\xi}) = \hat{\boldsymbol{r}} + \boldsymbol{\xi}$ with $\boldsymbol{r}$ is the 2n-dimensional vector of position and momentum operators $(\hat{X}_1, \ldots, \hat{X}_n; \hat{Y}_1, \ldots, \hat{Y}_n)$ and $\boldsymbol{\xi}$ is the classical displacement $(q_1, \ldots, q_n; p_1, \ldots, p_n)$. According to the relationship between the n moment and the characteristic function $\langle \boldsymbol{r}^n \rangle = \frac{1}{i^n} \frac{d^n \chi(\boldsymbol{\xi})}{d\boldsymbol{\xi}^n}|_{\boldsymbol{\xi}=0}$ then

$$\chi_S(\boldsymbol{\xi}) = \sum_{n=0}^{\infty} \frac{i^n}{n!} \cdot (\boldsymbol{\xi}^n \langle \boldsymbol{r}^n \rangle). \tag{A2}$$

By using the exponential expansion and taking the first two moments, we get

$$\chi_S(\boldsymbol{\xi}) = e^{-\frac{1}{2}\boldsymbol{\xi}^T \boldsymbol{\Gamma} \boldsymbol{\xi} + i\boldsymbol{\delta}^T \boldsymbol{\xi}}, \tag{A3}$$

where $\delta_j = \mathrm{tr}(\rho r_j)$ and $\Gamma_{jk} = \frac{1}{2}\mathrm{tr}(\rho\{\Delta r_j, \Delta r_k\})$, with $\Delta r_j = r_j - \delta_j$. The quadratic form of Eq. (A3) guarantees the Gaussian state, and the form of SLD is also quadratic. We can then assume the following expression for the SLD:

$$L = \boldsymbol{r}^T \boldsymbol{\Phi} \boldsymbol{r} + \boldsymbol{r}^T \zeta - \nu. \tag{A4}$$

Meanwhile, one can easily find that

$$\dot{\delta}_j = \frac{1}{2}\mathrm{tr}(\{L,\rho\}r_j) = \frac{1}{2}\mathrm{tr}(\rho\{L,r_j\}), \tag{A5}$$

$$\dot{\Gamma}_{jk} = \frac{1}{4}\mathrm{tr}(\{L,\rho\}\{r_j,r_k\}) = \frac{1}{4}\mathrm{tr}(\rho\{L,\{r_j,r_k\}\}). \tag{A6}$$

To calculate the traces above, we use the following partially symmetrically ordered characteristic function:

$$\begin{aligned}\chi_{\mathrm{P}}(\boldsymbol{\xi}_1,\boldsymbol{\xi}_2) &\equiv \frac{1}{2}\mathrm{tr}(\rho\{\mathrm{e}^{\mathrm{i}\boldsymbol{r}^{\mathrm{T}}\boldsymbol{\xi}_1},\mathrm{e}^{\mathrm{i}\boldsymbol{r}^{\mathrm{T}}\boldsymbol{\xi}_2}\}) \\ &= \chi(\boldsymbol{\xi}_1+\boldsymbol{\xi}_2)\cos(\frac{1}{2}\boldsymbol{\xi}_1^{\mathrm{T}}J\boldsymbol{\xi}_2).\end{aligned} \tag{A7}$$

$\partial_j^{(1,2)}$ represent the partial derivative with respect to the j-th element of $\boldsymbol{\xi}_{1,2}$, we have

$$\partial_\theta\delta_j = -\mathrm{i}\mathcal{L}^{(1)}\partial_j^{(2)}\chi_{\mathrm{P}}|_{\boldsymbol{\xi}_{1,2}=0}, \tag{A8}$$

$$\partial_\theta\Gamma_{jk} = -\mathcal{L}^{(1)}\partial_{j,k}^{(2)}\chi_{\mathrm{P}}|_{\boldsymbol{\xi}_{1,2}=0}, \tag{A9}$$

where

$$\mathcal{L} = -\sum_{n,m}\Phi_{mn}\partial_{mn} - \mathrm{i}\sum_l\zeta_l\partial_l - \nu. \tag{A10}$$

Substituting Eq. (A10) into Eqs. (A8) and (A9), then

$$\partial_\theta\delta_j = -\left(\sum_l\zeta_l\partial_l^{(1)}\right)\partial_j^{(2)}\chi_{\mathrm{P}}|_{\boldsymbol{\xi}_{1,2}=0} = \sum_l\Gamma_{jl}\zeta_l, \tag{A11}$$

$$\begin{aligned}\partial_\theta\Gamma_{jk} &= \left(\sum_{n,m}\Phi_{mn}\partial_{mn}^{(1)}+\nu\right)\partial_{jk}^{(2)}\chi_{\mathrm{P}}|_{\boldsymbol{\xi}_{1,2}=0} \\ &= [\mathrm{tr}(\Gamma\Phi)-\nu]\Gamma_{jk} + (2\Gamma\Phi\Gamma+\frac{1}{2}J\Phi J)_{jk},\end{aligned} \tag{A12}$$

where $J = \begin{pmatrix}0 & \mathbb{1}\\ -\mathbb{1} & 0\end{pmatrix} = -J^{\mathrm{T}} = -J^{-1}$ is the skew-symmetric matrix and $\mathbb{1}$ is the identity matrix. Due to the trace-preserving condition

$$\mathrm{tr}(L\rho) = \mathcal{L}\chi_{\mathrm{P}}|_{\boldsymbol{\xi}_{1,2}=0} = \mathrm{tr}(\Gamma\Phi)-\nu = 0, \tag{A13}$$

we have the following matrix forms:

$$\partial_\theta\delta = \Gamma\zeta, \tag{A14}$$

$$\partial_\theta\Gamma = 2\Gamma\Phi\Gamma - \frac{1}{2}J\Phi J^{\mathrm{T}}. \tag{A15}$$

This is an implicit matrix equation. One solution is to use canonical transform to take it into the diagonal representation. Here we define a matrix S satisfying $SJS^{\mathrm{T}} = J$, then

$$S\Gamma S^{\mathrm{T}} = \Gamma_d = \begin{pmatrix}\mathcal{D} & 0\\ 0 & \mathcal{D}\end{pmatrix}, \tag{A16}$$

where $\mathcal{D} = \mathrm{diag}(d_1,d_2,\ldots,d_n) \geqslant \mathbb{1}$ is a diagonal matrix. Since the covariance matrix Γ is canonical matrix

$$\begin{aligned}S\partial_\theta\Gamma S^{\mathrm{T}} &= 2S\Gamma JJ\Phi J^{\mathrm{T}}J^{\mathrm{T}}\Gamma S^{\mathrm{T}} - \frac{1}{2}SJJJ\Phi J^{\mathrm{T}}J^{\mathrm{T}}J^{\mathrm{T}}S^{\mathrm{T}} \\ &= 2S\Gamma(S^{\mathrm{T}}JS)J\Phi J^{\mathrm{T}}(S^{\mathrm{T}}J^{\mathrm{T}}S)\Gamma S^{\mathrm{T}} \\ &\quad -\frac{1}{2}SJ(S^{\mathrm{T}}JS)J\Phi J^{\mathrm{T}}(S^{\mathrm{T}}J^{\mathrm{T}}S)J^{\mathrm{T}}S^{\mathrm{T}},\end{aligned} \tag{A17}$$

then

$$\partial_\theta\Gamma_d = 2\Gamma_d\Phi_d\Gamma_d - \frac{1}{2}J\Phi_dJ^{\mathrm{T}}, \tag{A18}$$

where the defined symbol $\Phi_d = JSJ\Phi J^{\mathrm{T}}S^{\mathrm{T}}J^{\mathrm{T}}$, Notice that Γ_d and J are commuted with each other

$$\begin{aligned}\Gamma_d\partial_\theta\Gamma_d\Gamma_d &= 2\Gamma_d^2\Phi_d\Gamma_d^2 - \frac{1}{2}J\Gamma_d\Phi_d\Gamma_dJ^{\mathrm{T}} \\ &= 2\Gamma_d^2\Phi_d\Gamma_d^2 - \frac{1}{2}J\left(\frac{1}{2}\partial_\theta\Gamma_d + \frac{1}{4}J\Phi_dJ^{\mathrm{T}}\right)J^{\mathrm{T}} \\ &= 2\Gamma_d^2\Phi_d\Gamma_d^2 - \frac{1}{4}J\partial_\theta\Gamma_dJ^{\mathrm{T}} - \frac{1}{8}\Phi_d,\end{aligned} \tag{A19}$$

which can be solved explicitly

$$(\Phi_d)_{jk} = \frac{(\Gamma_d\partial_\theta\Gamma_d\Gamma_d + \frac{1}{4}J\partial_\theta\Gamma_dJ^{\mathrm{T}})_{jk}}{2d_j^2d_k^2-(1/8)}. \tag{A20}$$

An inverse symplectic transformation can transform it back to Φ. By putting Eq. (A10) into the definition of QFI, we have

$$\begin{aligned}I_{\mathrm{Q}} &= \mathrm{tr}(\rho L^2) = \mathcal{L}^{(1)}\mathcal{L}^{(2)}\chi_{\mathrm{P}}|_{\boldsymbol{\xi}_{1,2}=0} \\ &= \Bigg(\sum_{j,k,l,m}\Phi_{jk}\Phi_{lm}\partial_{jk}^{(1)}\partial_{lm}^{(2)} + \sum_{j,k}2\nu\Phi_{jk}\partial_{jk}^{(1)} \\ &\quad -\sum_{j,k}\zeta_l\zeta_k\partial_l^{(1)}\partial_k^{(2)} + \nu^2\Bigg)|_{\boldsymbol{\xi}_{1,2}=0} \\ &= \frac{1}{2}\mathrm{tr}(J\Phi J\Phi) + \mathrm{tr}(\Gamma\Phi\Gamma\Phi) + \mathrm{tr}^2(\Gamma\Phi) \\ &\quad -2\nu\mathrm{tr}(\Gamma\Phi) + \zeta^{\mathrm{T}}\Gamma\zeta + \nu^2 \\ &= \mathrm{tr}[(\Gamma\Phi\Gamma - \frac{1}{2}J\Phi J^{\mathrm{T}})\Phi] + \zeta^{\mathrm{T}}\Gamma\zeta \\ &= \mathrm{tr}(\partial_\theta\Gamma\Phi) + \partial_\theta\delta\Gamma^{-1}\partial_\theta\delta.\end{aligned} \tag{A21}$$

Now we take the covariance matrix of our model in this result, i.e., the single-mode optical output matrix $\sigma_{\mathrm{L,out}}$. Notice that the first moment of quantum fluctuations is zero in our model, it is necessary to know the expression of Φ in this case. Due to the canonical transformation requirements, we can take the matrix in the following form: $\sigma_d = \sqrt{\det\sigma}\,\mathbb{1}$ and $S = (\det\sigma)^{1/4}/\sqrt{\sigma}$. Using the inverse canonical transformation $S^{\mathrm{T}}\Phi_dS = S^{\mathrm{T}}JSJ\Phi J^{\mathrm{T}}S^{\mathrm{T}}J^{\mathrm{T}}S = \Phi$, we have

$$I_{\mathrm{Q}} = \frac{\mathrm{Tr}\left[S^{\mathrm{T}}\sigma_dS\partial_\theta\sigma S^{\mathrm{T}}\sigma_dS\partial_\theta\sigma + (1/4)S^{\mathrm{T}}JS\partial_\theta\sigma S^{\mathrm{T}}J^{\mathrm{T}}S\partial_\theta\sigma\right]}{2\det\sigma^2-(1/8)}, \tag{A22}$$

note that $J\partial_\theta\sigma J^{\mathrm{T}}\partial_\theta\sigma = \det\partial_\theta\sigma\,\mathbb{1}$, therefore

$$I_{\mathrm{Q}} = \frac{\mathrm{Tr}\left[S^{\mathrm{T}}\sigma_dS\partial_\theta\sigma S^{\mathrm{T}}\sigma_dS\partial_\theta\sigma + (1/4)\det\partial_\theta\sigma\,\mathbb{1}\right]}{2\det\sigma^2-(1/8)}. \tag{A23}$$

For the first term in the trace, notice that we only sum over diagonal elements and σ_d is diagonal, and then we have

$$\begin{aligned}
&\mathrm{Tr}\left[S^{\mathrm{T}}\sigma_d S\partial_\theta\sigma S^{\mathrm{T}}\sigma_d S\partial_\theta\sigma\right]\\
=\ &\mathrm{Tr}\left[(S^{\mathrm{T}}\sigma_d S\partial_\theta\sigma)^2\right]\\
=\ &\mathrm{Tr}\left[(S^{\mathrm{T}}J^{\mathrm{T}}S\sigma S^{\mathrm{T}}JS\partial_\theta\sigma)^2\right]\\
=\ &\mathrm{Tr}\left[(J^{\mathrm{T}}\sigma J\partial_\theta\sigma)^2\right]\\
=\ &\mathrm{Tr}\left[(J^{\mathrm{T}}\partial_\theta\sigma(\partial_\theta\sigma)^{-1}\sigma J\partial_\theta\sigma)^2\right]\\
=\ &\det\partial_\theta\sigma^2\mathrm{Tr}\left[((\partial_\theta\sigma)^{-1}\sigma)^2\right]. \qquad \text{(A24)}
\end{aligned}$$

The last step in the above equation uses the rotation property of trace, and finally we get

$$I_{\mathrm{Q}}(\theta)=\frac{\det\partial_\theta\sigma^2\mathrm{Tr}\left[((\partial_\theta\sigma)^{-1}\sigma)^2\right]+(1/2)\det\partial_\theta\sigma}{2\det\sigma^2-(1/8)}. \qquad \text{(A25)}$$

Acknowledgments

Project supported by the National Natural Science Foundation of China (Grant Nos. 11704205 and 12074206), the National Natural Science Foundation of Zhejiang Province (Grant No. LY22A040005), and K.C.Wong Magna Fund in Ningbo University.

References

[1] Pezzè L, Smerzi A, Oberthaler M K, Schmied R and Treutlein P 2018 *Rev. Mod. Phys.* **90** 035005
[2] Albarrán-Arriagada F, Alvarado Barrios G, Sanz M, Romero G, Lamata L, Retamal J C and Solano E 2018 *Phys. Rev. A* **97** 032320
[3] Zhou L K, Xu J H, Zhang W Z, Cheng J, Yin T S, Yu Y B, Chen R P, Chen A X, Jin G R and Yang W 2021 *Phys. Rev. A* **103** 043702
[4] Chen T, Kim J, Kuzyk M, Whitlow J, Phiri S, Bondurant B, Riesebos L, Brown K R and Kim J 2022 *IEEE Transactions on Quantum Engineering* **3**
[5] Rocheleau T, Ndukum T, Macklin C, Hertzberg J B, Clerk A A and Schwab K C 2010 *Nature* **463** 72
[6] Giovannetti V, Lloyd S and Maccone L 2004 *Science* **306** 1330
[7] Zheng Q, Yao Y and Li Y 2016 *Phys. Rev. A* **93** 013848
[8] Latune C L, Sinayskiy I and Petruccione F 2016 *Phys. Rev. A* **94** 052115
[9] Sanavio C, Bernád J Z and Xuereb A 2020 *Phys. Rev. A* **102** 013508
[10] Chen G, Zhang L, Zhang W H, Peng X X, Xu L, Liu Z D, Xu X Y, Tang J S, Sun Y N, He D Y, Xu J S, Zhou Z Q, Li C F and Guo G C 2018 *Phys. Rev. Lett.* **121** 060506
[11] Sanz M, Las Heras U, García-Ripoll J J, Solano E and Di Candia R 2017 *Phys. Rev. Lett.* **118** 070803
[12] Walter S, Nunnenkamp A and Bruder C 2014 *Phys. Rev. Lett.* **112** 094102
[13] Lian J, Liu N, Liang J Q, Chen G and Jia S 2013 *Phys. Rev. A* **88** 043820
[14] Flayac H, Minkov M and Savona V 2015 *Phys. Rev. A* **92** 043812
[15] Hoff U B, Kollath-Bönig J, Neergaard-Nielsen J S and Andersen U L 2016 *Phys. Rev. Lett.* **117** 143601
[16] Huang X, Zeuthen E, Vasilyev D V, He Q, Hammerer K and Polzik E S 2018 *Phys. Rev. Lett.* **121** 103602
[17] Ghosh S, Carney D, Shawhan P and Taylor J M 2020 *Phys. Rev. A* **102** 023525
[18] Peano V, Schwefel H G L, Marquardt C and Marquardt F 2015 *Phys. Rev. Lett.* **115** 243603
[19] Anetsberger G, Arcizet O, Unterreithmeier Q P, Rivière R, Schliesser A, Weig E M, Kotthaus J P and Kippenberg T J 2009 *Nat. Phys.* **5** 909
[20] Cheng J, Zhang W Z, Zhou L and Zhang W 2016 *Sci. Rep.* **6** 23678
[21] Zhang W Z, Cheng J, Li W D and Zhou L 2016 *Phys. Rev. A* **93** 063853
[22] Zhang W Z, Han Y, Xiong B and Zhou L 2017 *New J. Phys.* **19** 083022
[23] Cheng J, Liang X T, Zhang W Z and Duan X 2019 *Opt. Commun.* **430** 385
[24] Zhang W Z, Liang X T, Cheng J and Zhou L 2021 *Phys. Rev. A* **103** 053707
[25] Li W, Li C and Song H 2017 *Phys. Rev. E* **95** 022204
[26] Li W, Piergentili P, Li J, Zippilli S, Natali R, Malossi N, Di Giuseppe G and Vitali D 2020 *Phys. Rev. A* **101** 013802
[27] Li W, Es'haqi-Sani N, Zhang W Z and Vitali D 2021 *Phys. Rev. A* **103** 043715
[28] Li W 2022 *Phys. Rev. A* **106** 023512
[29] Huang P, Wang P, Zhou J, Wang Z, Ju C, Wang Z, Shen Y, Duan C and Du J 2013 *Phys. Rev. Lett.* **110** 227202
[30] Zhang W Z, Chen L B, Cheng J and Jiang Y F 2019 *Phys. Rev. A* **99** 063811
[31] Zhang W Z, Han Y, Xiong B and Zhou L 2017 *New J. Phys.* **19** 083022
[32] Ma Y, Danilishin S L, Zhao C, Miao H, Korth W Z, Chen Y, Ward R L and Blair D G 2014 *Phys. Rev. Lett.* **113** 151102
[33] Li X, Smetana J, Ubhi A S, Bentley J, Chen Y, Ma Y, Miao H and Martynov D 2021 *Phys. Rev. D* **103** 122001
[34] Armata F, Latmiral L, Plato A D K and Kim M S 2017 *Phys. Rev. A* **96** 043824
[35] Lassagne B, Garcia-Sanchez D, Aguasca A and Bachtold A 2008 *Nano Lett.* **8** 3735
[36] Naik A K, Hanay M S, Hiebert W K, Feng X L and Roukes M L 2009 *Nat. Nanotech.* **4** 445
[37] Pontin A, Lang J E, Chowdhury A, Vezio P, Marino F, Morana B, Serra E, Marin F and Monteiro T S 2018 *Phys. Rev. Lett.* **120** 020503
[38] Toroš M and Monteiro T S 2020 *Phys. Rev. Res.* **2** 023228
[39] Davuluri S, Li K and Li Y 2017 *New J. Phys.* **19** 113004
[40] Li K, Davuluri S and Li Y 2018 *Science China Physics, Mechanics Astronomy* **61** 90311
[41] Li K, Davuluri S and Li Y 2018 *Chin. Phys. B* **27** 084203
[42] Davuluri S 2016 *Phys. Rev. A* **94** 013808
[43] Li K, Davuluri S and Li Y 2018 *Chin. Phys. B* **27** 084203
[44] Law C K 1995 *Phys. Rev. A* **51** 2537
[45] Giovannetti V and Vitali D 2001 *Phys. Rev. A* **63** 023812
[46] Genes C, Vitali D, Tombesi P, Gigan S and Aspelmeyer M 2008 *Phys. Rev. A* **77** 033804
[47] Genes C, Mari A, Tombesi P and Vitali D 2008 *Phys. Rev. A* **78** 032316
[48] Helstrom C 1968 *IEEE Transactions on Information Theory* **14** 234
[49] Helstrom C W 1967 *Information and Control* **10** 254
[50] Braunstein S L and Caves C M 1994 *Phys. Rev. Lett.* **72** 3439
[51] Jiang Z 2014 *Phys. Rev. A* **89** 032128
[52] Thompson J, Zwickl B, Jayich A, Marquardt F, Girvin S and Harris J 2008 *Nature* **452** 72